Investigation of Tip-leakage-vortex Breakdown and Its Role in Rotating Stall in a 1.5-stage Low-speed Axial-compressor

Xiang HE[1,2], Hongwei MA[1*] and Wei WEI[1]

ISROMAC 2016

International Symposium on Transport Phenomena and Dynamics of Rotating Machinery

Hawaii, Honolulu

April 10-15, 2016

Abstract

A whole-annulus unsteady numerical simulation is carried out to investigate the mechanism of the rotating stall in a 1.5-stage low-speed axial-compressor. By comparing the experimental and numerical results, the numerical results are validated. The numerical simulation captures the most features of the rotating stall of the 1.5-stage compressor observed from the experimental results. The unsteady bubble-like breakdown appears in the tip leakage vortex at the near stall condition. With the compressor throttling, the modal wave appears, increases in intensity and induces the part of the breakdown-vortex flow spilled over the adjacent blade leading-edge unsteadily, which form a spike. Consequently, the spikes emerge around the compressor annulus at the same time and the intensity and size of the spikes is increased rapidly during the inception period. At last, the spikes are merged into a large stall cell, which propagates around the annulus with 30% rotor speed.

Keywords

axial compressor — tip-leakage-vortex breakdown — rotating stall — stall inception

[1] *National Key Laboratory of Science and Technology on Aero-Engines*
Collaborative Innovation Center of Advanced Aero-Engine,
School of Energy and Power Engineering, Beihang University, Beijing, 100191, China

[2] *China Aviation Powerplant Research Institute, Zhuzhou 412002, China*

*__Corresponding author__: mahw@buaa.edu.cn

INTRODUCTION

Compressor stall/surge usually leads to significant loss in performance, engine flameout, even serious mechanical failure. Therefore, many efforts were devoted to reveal the mechanisms of compressor stall and then the designers develop effective stall/surge control method to extend the stable operating range of compressor.

It is well known that the rotating stall is usually triggered by the flow disturbances, usually named by stall inception. In the past two decades, two distinct stall-inception patterns had been identified. The first one refers to modal wave [1,2,3], which belongs to a long-length-scale/modal disturbance. The second one is usually called spike inception or the short length-scale disturbance, which was observed initially by Day [4].

Many research works indicate that the spike inception may be linked to the phenomena of unsteady tip flow which usually happen at the near-stall operating condition. Variety of unsteady-tip-flow phenomena was discovered in the low-speed axial compressor, including tip separation vortex[5,6], tip-leakage-vortex breakdown[7,8], tornado-like separation vortex[9] and tip-leakage-vortex oscillation[10,11].Actually, the phenomenon of the unsteady tip flow is more complicated in a transonic axial-compressor because of the existence of the shock wave-boundary layer interaction, which can refer to [12-14].All these results cannot clarify the relationship between the unsteady tip flow and the spike inception. However, Vo et al.[15] answered this question and believed that the criteria of spikes include two aspects which are tip clearance flow spilling over the adjacent blade leading-edge and the impingement of the tip clearance backflow on the pressure surface below blade tip, which built a relationship between the tip clearance flow and stall inception.

Nomenclature

BPF	Blade passing frequency
FMR	Frequency mixing region
IGV	Inlet guide vanes
LLAC	Low-speed Large-scale Axial Compressor
PIV	Particle image velocimetry
PS	Pressure surface or pressure side
SS	Suction surface or suction side
TLV	Tip leakage vortex
TLF	Tip leakage flow
BPF	Blade passing frequency

Due to the rapid advance of high-performance computing in the past ten years, the full-annulus 3D unsteady computation can be used to simulate the phenomena of compressor rotating stall. Gourdian et al.[16] and Chen et al.[17] carried out a full-annulus 3D numerical simulation respectively in low and high speed compressor and the results support the Vo's spike stall criteria, but their discussion don't reveal the mechanism of the tip clearance flow spillage. Pullan et al.[18] investigate the origins and structure of spike rotating stall in multiple axial-compressors. High incidence results in a separation vortex shedding from the leading edge in the tip region and the separation vortex belongs to a tornado-like separation vortex as was suggested by Inoue et al. The upper end of the tornado-vortex moves circumferentially along the casing and leads to a new separation on the next blade. This flow features describe the process of the spike formation and

propagation and reveal the mechanism of the unsteady tip flow spillage. Moreover, Wu et al.[6] also carried a 3D full-annulus numerical simulation in a low-speed axial-compressor and expose that the spillage of the unsteady tip separation vortex is another mechanism of the spike stall inception.

In recent years, more and more experimental and numerical results focus on studying the role of the unsteady tip flow in spike inception to reveal its mechanism. Current work also focuses on this issue and attempts to provide some results to improve understanding of the relationship between unsteady tip leakage flow and spike inception in a low-speed axial-compressor.

The organization and scope of the paper is as follows. Firstly, the compressor facility and numerical method are introduced and the simulation results are validated. Secondly, the features of the leakage vortex breakdown are investigated through comparative analysis of the numerical and experimental results and the relationship between leakage vortex breakdown and the stall inception is revealed. At last, the transit process of rotating stall is described and discussed in detail.

1. EXPERIMENTAL AND NUMERICAL METHOD

1.1 Experimental facility

The Low-speed Large-scale Axial Compressor (LLAC) test rig is a single-stage axial compressor with inlet guide vanes (IGV), shown in Figure 1. The rotor and stator blades with C4 series airfoil are designed in terms of the free vortex law. More detailed design parameters are summarized in Table 1. Because the past measurements show that the typical rotor speed is 75% corrected rotor speed, the discussions in this paper are focus on the condition of n=900rpm.

Table 1 compressor characteristics

Casing diameter	1 m
Hub-to-tip ratio	0.6
Number of IGV blades	36
Number of rotor blades	17
Number of stator blades	20
Design speed	1200 r/min
Rotor tip gap	3mm (1.5%)
Re_{chord}	7.5×10^5

1.2 Numerical method

The whole-annulus steady and unsteady numerical simulations were carried out in this 1.5-stage low-speed axial-compressor. The length of the inlet and outlet computational domains is respectively 0.5 and 1 times of the casing diameter. The mesh was generated with the Turbogrid software and the grid topology is HOH as shown in Figure 1. The number of mesh points for one passage is about 200 000 for the rotor channel, 90 000 and 170 000 for one IGV and stator channel. The rotor tip clearance is taken into account with the H-mesh of 10 points in the radial direction. Total mesh number is 10 000 000. The nodes distribution is described in Table 2.

The unsteady flow field is simulated using the CFX code to solve the viscous Reynolds-averaged Navier-Stokes equations with the time pursuing finite volume method. The space discretization is made by the second order upwind scheme. The turbulence model was chosen in the numerical simulation, coupled with a scalable wall functions ($y^+\approx20$). For this application, 340 iterations are required to simulate one revolution of the rotor, 20 iterations for one channel. Each physic time step includes 10 virtual time steps which can make sure the simulation convergence.

The rotor speed is fixed at the nominal rotor speed of 900rpm. Uniform stagnation pressure and temperature are respectively 101325Pa and 288.15K given as the inlet boundary conditions. The inlet flow angle and turbulence intensity is respectively 0° and 5%. The outlet boundary condition is imposed as the average static pressure at the stable operating points, which meet the radial equilibrium condition. In order to simulate the process of compressor stall, a throttle model is applied at the outlet. The static pressure Psout is determined via the Eq.1.

$$Ps_{out} = Pt + \frac{1}{2}\times\frac{K_0}{K_1}\times\rho\times V_{axial}^2 \quad (1)$$

Where, Pt is atmosphere pressure, Vaxial is the axial velocity, ρ and K0 are constants. With these conditions, all points of the compressor characteristic can be simulated. The position of the operating point on the characteristic is determined only by the value of the throttle parameter K1.

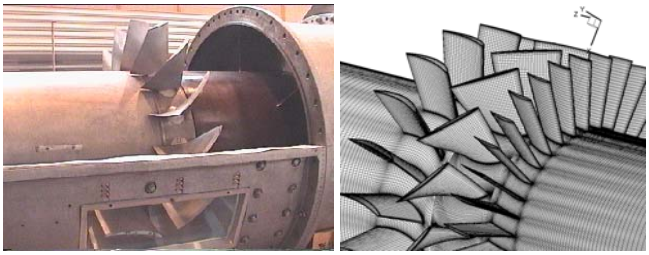

Figure 1. Partial view of the rig and the 3D mesh

Table 2 Mesh distribution of the 1.5-stage compressor (Unit: K)

IGV	Rotor	Stator	Total
3200/90	3400/200	3400/170	10000

1.3Validity of numerical simulation

The overall compressor performance in terms of the static-to-static pressure rise coefficient ($\Psi=\triangle Ps/0.5\rho Utip2$) and the flow coefficient ($\Phi=Vx/Utip$) was measured with circumferential array of four static pressure taps on the casing at both inlet and outlet of the compressor, as shown in Figure 2a. Agreement between static pressure rise of steady simulation and experimental results is good. The discrepancy is also not very large between unsteady computational results and experimental ones. After imposing the throttle model on the outlet at the near stall condition, the stall process was simulated and the dynamic static pressure rise performance was obtained as shown.

Figure 2b shows the total pressure coefficient range from

50% to 100% span measured by the five-hole probe at the design operating condition. By comparing numerical and experimental results, it indicates that the discrepancy is not very large.

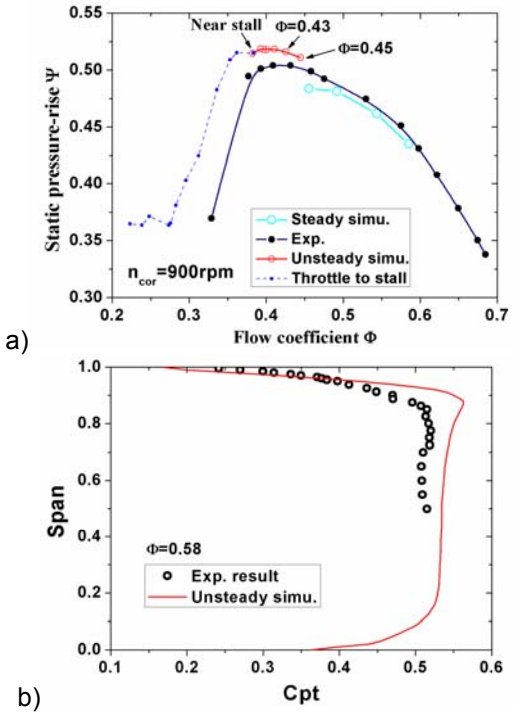

Figure 2. a)static pressure-rise performance，b)span-wise distribution of total pressure downstream of rotor at design operating condition

Four dynamic sensors, P0~P3, are located around the annulus on the casing at 10% chord upstream of the rotor leading-edge. The compressor was throttled to stall from near stall operating condition (Φ=0.37) and the data acquisition system records the dynamic pressure signals with the sampling rate of 12 kHz, as shown in Figure 3a. The modal waves can be clearly observed from the pressure traces at the pre-stall period from -8 to 0 revolutions. It propagates around the annulus with 20% rotor speed. Many shaft order perturbations, which are induced by the rotor asymmetries and propagate around the annulus at 100% rotor speed, appears at the modal peaks, while it decays very fast at the through of the modal wave [19]. At -2 revolutions, the shaft order perturbation evolve into a spike inception (disturbance), marked with 'A', and its propagation speed is reduced to below 80% rotor speed. In the range of 0 to 5.5 revolutions, many short-scale disturbances are produced by the modal wave and increase in size and amplitude, namely the frequency mixing region (FMR, marked with red dashed line) suggested by NIE Chaoqun [20]. At about 5~6 revolutions, these disturbances are merged into a large stall cell and the compressor comes into the full stall condition. Only one stall cell can be observed and its propagation speed is 30% rotor speed. It should be noted that the modal wave grows into the stall cell smoothly, which agrees well with the conclusions obtained by NIE [20]. That means the stall is triggered by modal wave rather than a spike.

Figure 3b shows the monitoring pressure traces obtained from the numerical simulation. The locations of the monitoring points are the same as experimental ones. Modal wave with 20% rotor speed was captured by the numerical simulation as indicated in Figure 4, but its amplitude is obviously lower than the BPF. Therefore, it is hardly observed from the pressure traces during the prestall period in the range of 0 to 3 revolutions. At about 3.2 revolutions, the spike inception firstly appears in pressure signals C1. Consequently, many spikes emerge around the compressor annulus at the same time and the intensity and size of the spikes is increased rapidly during the inception period in the range of 3 to 5 revolutions, which indicate the compressor comes into FMR. At last, the spikes are merged into a large stall cell, which propagates around the annulus with 30% rotor speed. These imply that the numerical simulation almost captures the most features of the rotating stall of the 1.5-stage compressor observed from the experimental results.

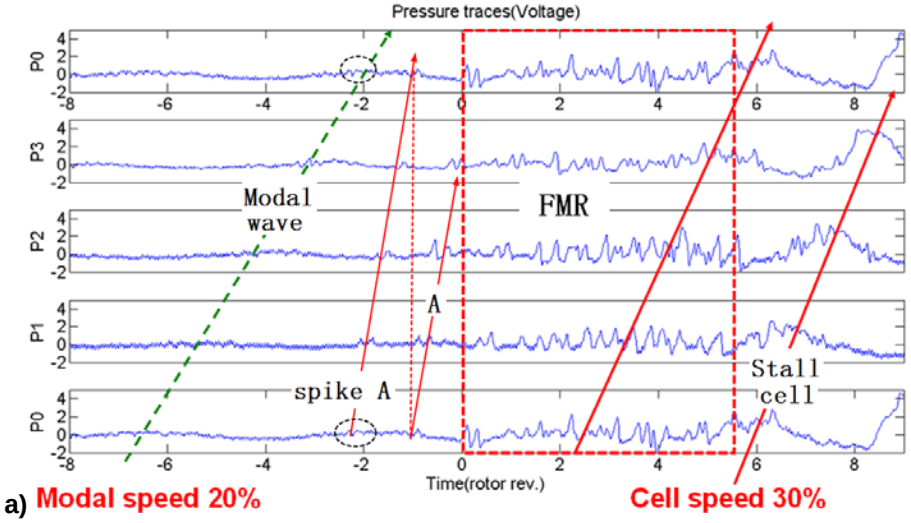

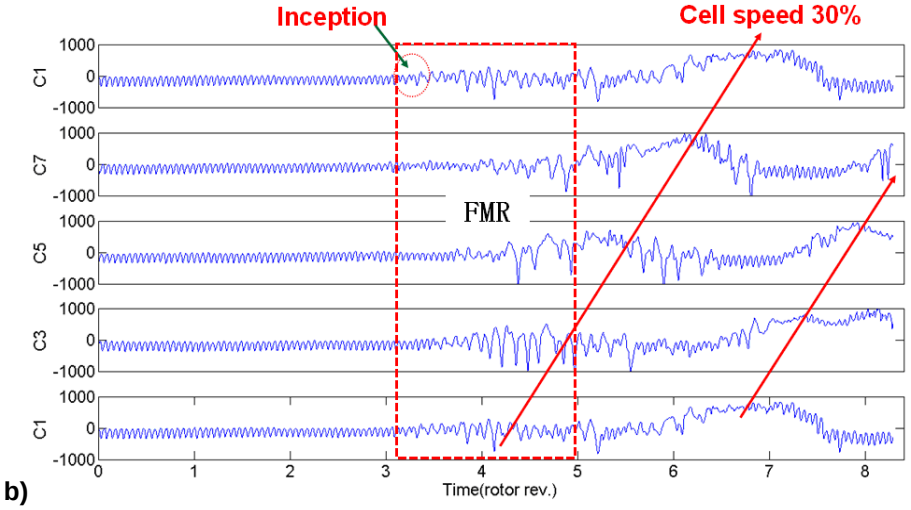

b)

Figure 3 Circumferential propagation of the stall inception and stall cell，a)numerical simulation, b)experimental results

.

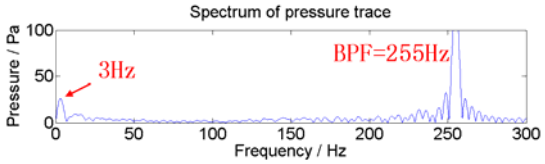

Figure 4 FFT spectrum of the numerical signal of C3 range 0~3rev. in Figure 3b

2. Analysis of the numerical results

2.1 Leakage vortex breakdown and stall inception

To understand the mechanism of stall inception observed from pressure traces in Figure 4, the complicated tip flow is visualized and investigated by analyzing the numerical results in detail.

Figure 5 shows two instantaneous contours of the normalized vorticity which is defined by $\tilde{\omega}=\omega/2\Omega$ whereω is absolute vorticity and $\Omega$is the rotor angular velocity. The leakage vortex corewiththe concentrated vorticity can be observed clearly in the range of leading-edge to 30% chord suction-side cross-section. This corresponds to the strong rolling-up of the vortex shown by a spiraling of the leakage streamlines. However, the concentrated vorticity decreases rapidly downstream of the 40% chord suction-side cross-section, which means the leakage vortex core expansion. The isosurface of W/Vtip=0.1 marked with A and B show the recirculation region exists in the tip passage as indicated in Figure 5. Consequently, the recirculation region A increases in scale and moves toward to pressure side of the adjacent blade leading-edge. Through observing the distributions of streamlines in detail, it is found that the recirculation region B seems to decrease in intensity and moves along the pressure side. Actually, there is a stagnation point in the center of the recirculation region B where the relative velocity is almost zero as shown in Figure 6. The flow features of stagnation point, the recirculation and the concentrated vorticity dissipation agree well with Inoue's conclusions. It indicates that such recirculation region belong to an unsteady flow phenomena of bubble-like tip-leakage-vortex breakdown.

Actually, many experimental results, including unsteady pressure, LDV[21,22] and PIV measurements[23],validate that the phenomena of tip-leakage-vortex breakdown occurs at about 30% axial chord(or about 60% chord suction-side cross-section) in this 1.5-stage axial-compressor for the 0.5% tip gap configuration at the near stall condition. For the current 1.5% tip gap configuration, Zhang et al demonstrate detailed PIV experimental results in [24]. Flow stagnation and flow reverse sometimes appears in the tip-leakage-vortex core at about downstream 70% chord suction-side cross-section. Moreover, the tip-leakage-vortex core expands abruptly and losses the concentration features at this cross section. These flow features indicate the TLV breakdown occurs at about the 70% chord suction-side cross-section for the current 1.5% tip gap configuration as shown in Figure 6b.Comparing with Figure 6b, Figure 6a shows that the TLV breakdown in the numerical result also occursat the same cross section. Because the numerical operating condition of the numerical simulation is closer to stall condition than the experimental operating condition, the influence scope is obvious larger than the later and the stagnation point is closer to the leading-edge plane.

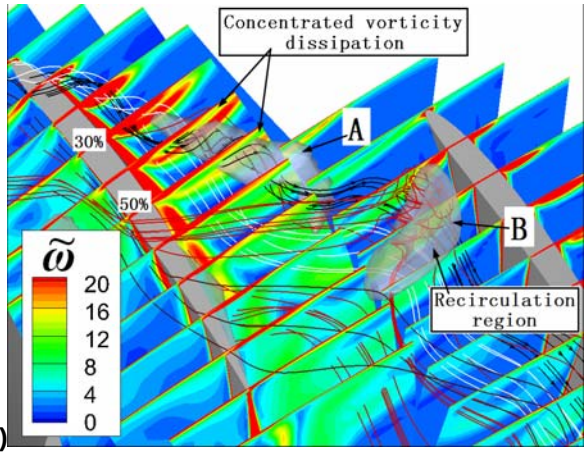

a)

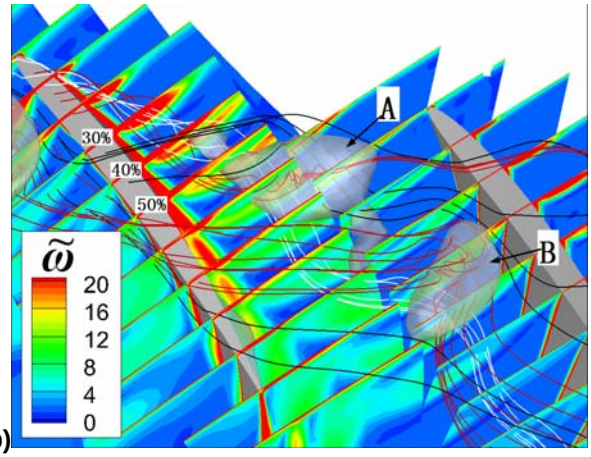

b)

Figure 5 Distributions of normalized vorticity, streamlines and the velocity isosurface of W/Vtip=0.1 at about 1.5 revolutions

With the compressor throttling the stall inception appears at about 3.2 revolutions as shown in Figure 3b. The following section will discuss the relationship between the leakage vortex breakdown mentioned above and the stall inception in detail.

Figure 7 indicates that the concentrated vorticity dissipation occurs downstream of 30% chord suction-side cross-section, which means the location of the leakage vortex breakdown moves upstream with throttle closing. After the leakage vortex breakdown, a very large recirculation vortexmarked with B was formed in the middle of the passage and the low-velocity flow was spilled over the adjacent blade leading-edge. Such condition can be observed more clearly in Figure 7b. It implies that a stall inception was triggered by the unsteady leakage vortex breakdown. In the later, the same phenomena will happens in the right passage. Therefore, the stall inception propagates along the compressor annulus in the opposite rotating direction.

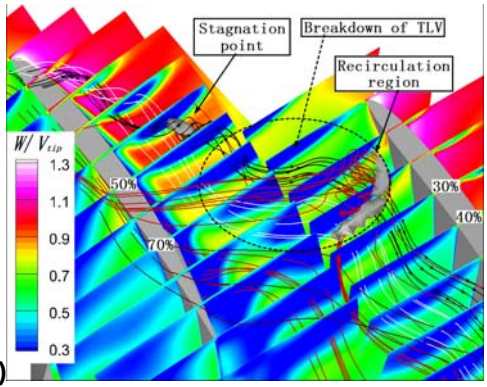

a)

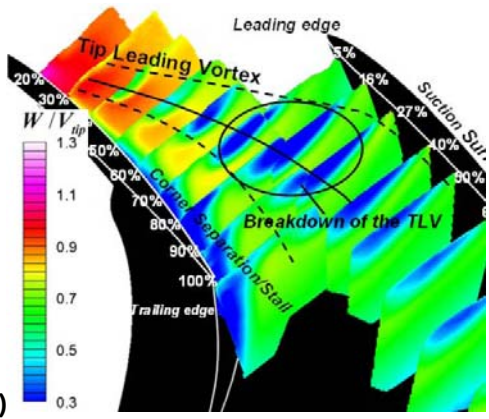

b)

Figure 6 Relative velocity distributions, a) instantaneous numerical result, b) averaged PIV result [24]

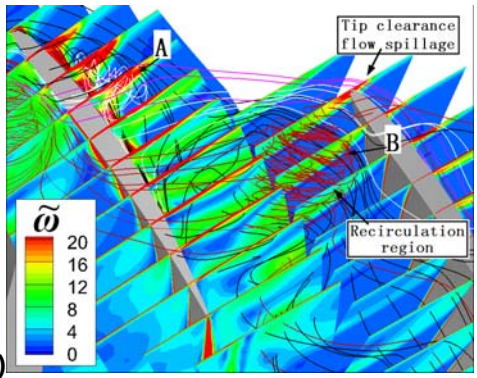

a)

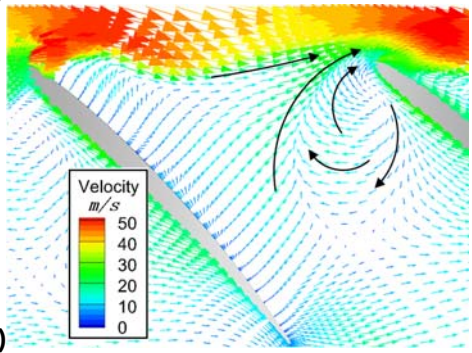

b)

Figure 7 Leakage flow spillage leading to stall inception at 3.24 revolutions, a) normalized vorticity and streamlines distributions in tip region, b) Tangential velocity vector distribution at 98% span

2.2 Development of the stall cell

The tip leakage flow mixes after leaving the tip gap, has higher entropy than the incoming flow [15]. Therefore, the high entropy gradient region can be used to track the incoming/tip leakage flow interface. With the flow coefficient decreasing, the interface move toward the rotor leading-edge plane.

Contours of entropy rise on the rotor leading-edge plane are shown in Figure 8. Figure 5 and 6 shows clearly that the incoming/tip leakage flow interface is almost aligned with the leading-edge plane at the near stall condition. Such case also can be observed from Figure 8a and the high entropy rise region appears on the leading-edge plane at the tip region.

With the compressor keeping on throttling, the phenomena of the leading-edge tip-leakage-flow spillage

occurs at least five circumferential locations, marked with the letters of A-D, as shown in Figure 8b. Here, the blade C is corresponding to the left blade in Figure 7.

Consequently, the size of the spikes is increased to half of span as shown in Figure 8c. One of them occupies 2~3 rotor passages, which indicates the small stall cell is formed marked with dashed red oval ring. At last, these spikes are merged into a large full-span stall cell and the influence region is almost half of the compressor annulus.

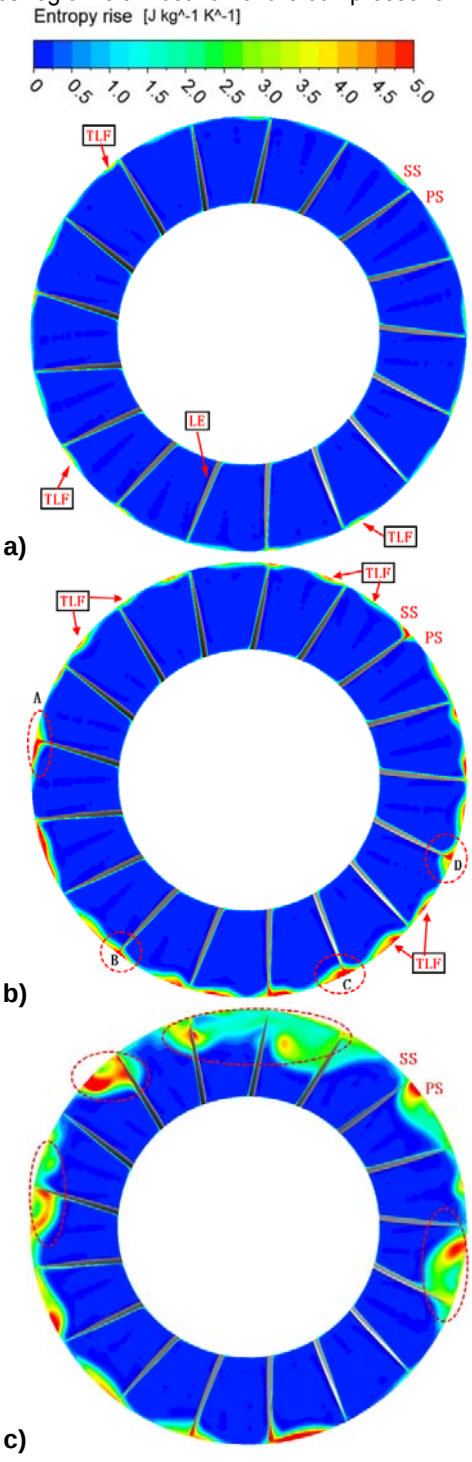

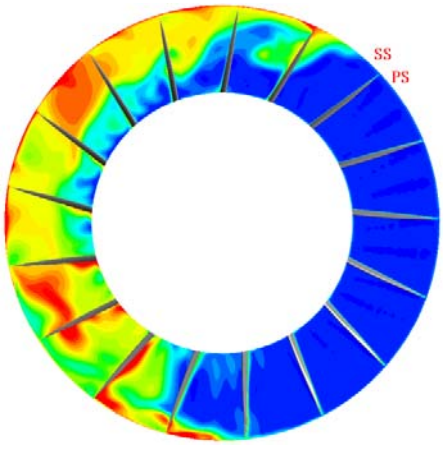

Figure 8 Evolvement of the stall cell, a)1.5rev., b)3.24rev., b)4.4rev., d)7rev.

2.3 Full stall

At the full stall condition, about 6 passages keep stable, which the local flow coefficient is about 0.43 (near mid-operating condition away from stall condition), but other passages are stalled as observed from the entropy-rise contours in Figure 8d and 9. Such situation can be explained by Cumpsty's words [25]: 'Rotating stall is a mechanism which allows the compressor to adapt to a mass flow which is too small: instead of trying to share the limited flow over the whole annulus the flow is shared unequally, so that some blade passages (or parts of passages) have a quite large flow and some very little'.

Because of existence of the IGV, no large-scale recirculation vortex can be seen in the stalled region upstream of the rotor leading-edge plane but a high entropy rise region, which indicates a reversed flow, can be observed clearly in the IGV passages as shown in Figure 9 b and c.

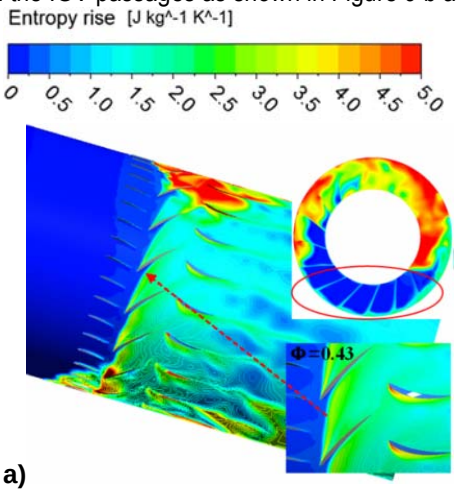

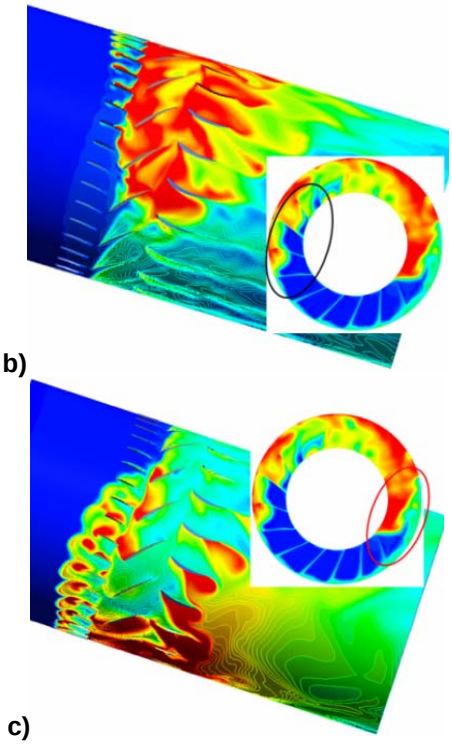

Figure 9 Instantaneous entropy distributions at 98% span at 7.4 revolutions

3.Conclusions

A whole-annulus unsteady numerical simulation is carried out to investigate the rotating stall process in a 1.5-stage low-speed axial-compressor. Some conclusions are summarized as following:

By comparing the measured and monitored pressure signals in experiments and simulations respectively, it clearly demonstrates that current numerical results capture the most features of the rotating stall process of the 1.5-stage compressor.

A modal wave was measuredat the near stall operating condition. It was also captured by numerical simulation, though its intensity is slightly lower than the measured one.

Unsteady tip-leakage-vortex breakdown occurs in the rotor blade tip region at the near stall condition. Once the unsteady tip leakage flow is spilled over the adjacent blade leading-edge, the spike inception is triggered.

Many small-scale disturbances are induced by the modal wave in the frequency mixing region and the numerical results verify that these small disturbances are actually the spikes.

These spikes emerge around the rotor annulus almost at the same time and the intensity and size of the spikes is increased rapidly during the inception period.

At last, the spikes are merged into a large stall cell, which propagates around the annulus with 30% rotor speed. The number and propagation speed of the stall cell is well predicted by the simulation.

Acknowledgement

This work is funded by the National Natural Science Foundation of China, Grant No.51161130525, 51136003, and the 111 Project, No.B07009.

References

[1] Moore, F. K., and Greitzer, E. M., 1986, A theory of post-stall transients in axial compression systems: Part 1- Development of equations, Part 2- Application, ASME Journal of Engineering for Gas Turbines and Power, Vol.108, pp.68-76, pp.231-239

[2] McDougall, N. M., Cumpsty, N. A., and Hynes, T. P., 1990, Stall inception in axial compressors, ASME Journal of Turbomachinery, Vol.112, pp.116-125

[3] Garnier et al. Rotating waves as a stall inception indication in axial compressor, ASME Journal of Turbomachinery, Vol.113, pp.390-301

[4] Day, I. J., 1993, Stall inception in axial flow compressors, ASME Journal of Turbomachinery, Vol.115, pp.1-9

[5] Marz J., Chunill Hah and Wolfgang Neise. An experimental and numerical investigation into the mechanisms of rotating instability. Journal of Turbomachinery, 2002, 124:367-375

[6] Yanhui Wu, Qingpeng Li, JiangtaoTian, and Wuli Chu. Investigation of pre-stall behavior in an axial compressor rotor, Part 1: Unsteadiness of tip clearance flow, Part 2: Flow mechanism of spike emergence. Journal of Turbomachinery, 2012, 134

[7] Furukawa M., Saiki K., Nagayoshi K. et al. Effects of Stream Surface Inclination on Tip Leakage Flow Fields in Compressor Rotors.Journal of turbomachinery, 1998, 120:683-692.

[8] Furukawa M., Inoue M., Saiki K.and Yamada K.The role of tip leakage vortex breakdown in compressor rotor aerodynamics. Journal of Turbomachinery, 1999, 121:469-480

[9] Inoue M., et al. Effect of tip clearance on stall evolution process in a low-speed axialcompressor stage. ASME Paper, GT-2004-53354

[10] Mailach R, Sauer H, Vogeler K. The periodical interaction of the tip clearance flow in the blade rows of axial compressors. ASME Paper, 2001 GT-0299, 2001

[11] Hongwu Zhang, Xiangyang Deng, Feng Lin, et al. A study on the mechanism of tip leakage flow unsteadiness in an isolated compressor rotor. ASME Paper GT2006-91123

[12] Yamada F. and Funazaki.The behavior of tip clearance flow at neastall condition in a transonic axial compressor orotor [C]. ASME GT2007-27725

[13] Hah C., Bergner and Schiffer. Tip clearance vortex oscillation, vortex shedding and rotating instabilties in an axial transonic compressor rotor [C]. ASMEGT2008-50105

[14] Juan Du, Feng Lin, Hongwu Zhang, et al. Numerical investigation on the self-induced unsteadiness in tip leakage flow for a transonic fan rotor[J]. Journal of Turbomachinery, 2010, 132

[15] Vo H. D., Tan C. S., and Greitzer E. M. Criteria for spike initiated rotating stall.Journal of Turbomachinery, 2008, 130

[16] Gourdain N., Burguburu S., Leboeuf F., et al. Simulation of rotating stall in a whole stage of an axial compressor. Compputers& Fluids, 2010, 39:1644-1655

[17] Chen J. P., Hathawary M. D. Herrick G. P. Prestall behavior of a transonic axial compressor stage via time-accurate numerical simulation. Journal of Turbomachinery, 2008, 130

[18] Pullan G., Young A., Dayl., et al. Orgins and structure of spike-type rotating stall. ASME GT2012-68707

[19] HE Xiang, MA Hongwei and ZHANG Jun. Wavelet analysis of the shaft order perturbation and stall inception in an axial compressor. Journal of Thermal Science, 2013, 22(3):223-228.

[20] NIE Chaoqun, CHEN Jinyi, JIANG Haokang and XU Lipin. Experimental investigation on inception of rotating stall in a low-speed axial compressor. Journal of engineering thermophysics, 1998, 19(3). (In Chinese)

[21] Ma Hongwei and Jiang Haokang. Three-Dimensional Turbulent Flow Of The Tip Leakage Vortex In An Axial Compressor Rotor Passage. ASME2000-GT-503.

[22] Ma Hongwei and Jiang Haokang. Three-Dimensional Turbulent Flow in the tip region of an axial compressor rotor passage at a near stall condition. ASME 2001-GT-0331

[23] Baojie Liu, Xianjun Yu, Huoxing Liu, et al., 2006, “Application of SPIV in Turbomachinery”, Experiments in Fluids, 40, pp.621-642

[24] Zhibo Zang, Xianjun Yu and Baojie Liu. Characteristics of the tip leakage vortex in a low-speed axial compressor with different rotor tip gaps. ASME GT2012-69148

[25] Cumpsty N. A. Compressor aerodynamics. Longman Group, 1989, pp.360